Dottorato di ricerca in Fisica - XXXII ciclo
Report attività

Pasquale Digregorio
Tutor: Prof. Giuseppe Gonnella

The PhD project has concerned the characterization of the phase diagram of two different models of active Brownian particles (ABP) in two spatial dimensions: the self-propelled disks model and the self-propelled dumbbells model. During the last three years we have been characterized the complete phase transition diagram of these two models, which evolve out of thermal equilibrium, in the $(\mathrm{Pe} - \phi)$ parameter space. In this report, we summarize all the most significant features of these two models and compare them as two different, though both paradigmatic, examples of motile particles.

- We have been found few remarkable differences between the two phase diagrams, concerning the nature of motility-induced phase separation (MIPS) and the way the melting scenario and the equilibrium stable phases are affected by the presence of activity;
- for disks the two-stage melting passive scenario with a first order phase transition between liquid and hexatic and a BKT transition between hexatic a solid is maintained up to small values of activity. All the three pure phases survive as stable phases up to very high activities. Moreover, the existence of an "active hexatic" phase and an "active solid" one plays a crucial role in recognizing the nature of the coexisting phases in MIPS;
- this behavior suggested us to proceed further in studying the similarity of our system with its passive counterpart, with a careful characterization of out-of equilibrium transitions in terms of the population of topological defects and their large-scale behavior;
- for dumbbells we observe a macroscopic coexistence between hexatically ordered regions and disordered ones over a finite interval of packing fractions, for all activities. In the passive limit, this interval remains finite, aw with the disks, but, differently from them, we didnt find discontinuous behavior upon increasing activity from the passive limit.

We present in this report a short review of the theoretical background of the work, before presenting all the details of our numerical study and the conclusions that we have collected.

1. Introduction

The phrasing *active matter* has became a widely used term to refer to all physical systems in which the constituents are able to perform self-sustained motion, extracting energy from either internal storage or external surroundings. This is actually a formal description of the way that living systems use to move, exploring their surroundings. A collection of self-propelled particles is intrinsically out-of-equilibrium. However, a subtle difference exists between active matter and other classical examples of non-equilibrium systems in how non-equilibrium takes place. While suitable boundary conditions or external fields, like for example applied shear stresses or temperature gradients can simply drive the system out of thermodynamic equilibrium, in active systems non-equilibrium arises at the level of each single active component of the system, breaking detail balance [1]. As a consequence of this feature, active systems display a richer phenomenology than their passive counterparts, as the one observed in living systems of large animals [2, 3], bacteria [4], or in synthetic ones [5, 6]. Among others, Active Brownian Particles (ABP) models constitute standard paradigmatic models to study the impact of activity on soft matter [7, 8, 9]. For many of the active systems cited above, self-propulsion is able to trigger a motility-induced phase separation (MIPS) between a low-density gas-like phase and dense stable aggregates [10], reminiscent of the equilibrium liquid-gas transition but in the absence of cohesive forces and without a thermodynamic framework to support it [11, 12].

It is worth saying that the most intriguing phenomena induced by activity, as well as the most promising experimental applications, concern systems confined in 2D layers. Being interested in further exploring aggregation phenomena and thermodynamic phases of passive and active two-dimensional systems at any finite density [13, 14, 15] and trying to establish a reference phase diagram for active matter, we naturally faced the long debated problem, still not fully understood, of melting transitions in two dimensions.

While phase transitions in 2D systems with short-range interactions do not involve any spontaneous symmetry breaking mechanism [16], also ordered crystal-like phases have long been

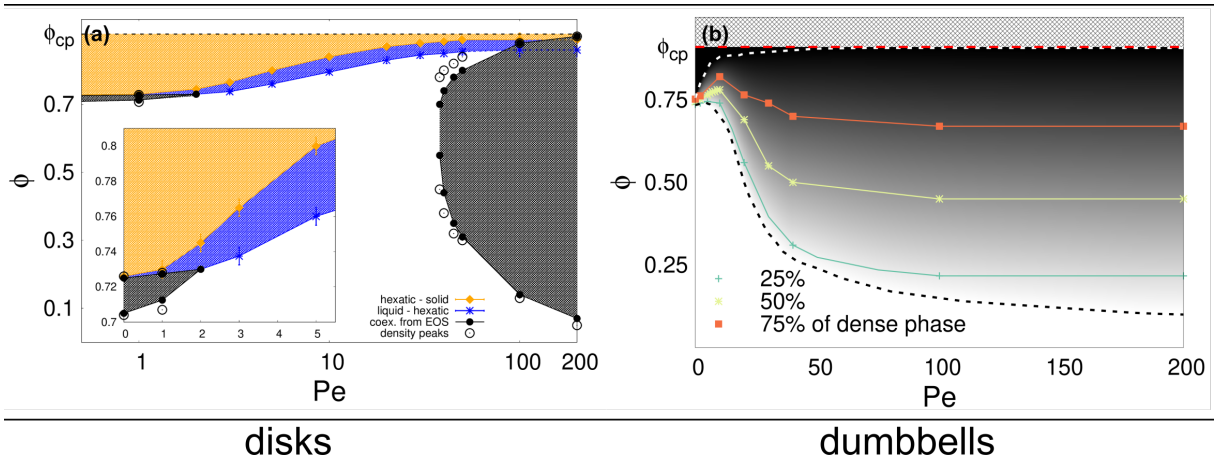

Figure 1. (a) Phase diagram of active brownian disks evolving according to Eq. 1. Figure adapted from [25]. Black empty circles and filled symbols are used to show the limits of the co-existence region inferred, respectively, from density pdfs and the equation of state. Orange points indicate solid-hexatic transition, solid region is colored in orange. Blue region is the hexatic region and blue points indicate hexatic-liquid transition. In the inset, enlargement of the small activity region across the coexistence. (b) Phase diagram of active brownian dumbbells (see Eq. 3), adapted from [26]. The grey scale represents the amount of dense ordered phase in the system. The dotted curves are the location of the lower (in black) and upper (in white) limits of coexistence. In the black region above the white dotted line the system is in a single ordered phase. The solid coloured line-points indicate curves on which there is a constant proportion of areas covered by the dense and dilute phases in the coexistence region (see the key).

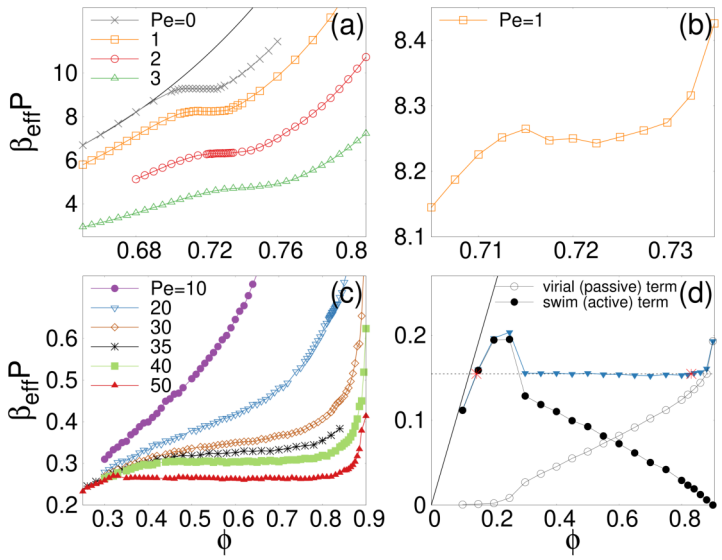

Figure 2. Equation of state. (a) Values of the pressure computed according to 4 for low Pe and analytical form for passive hard disks (continuous line). (b) Details around the liquid-hexatic coexistence region for Pe= 1. (c) Intermediate Pe regime. (d) Swim $P^{\rm swim}$ act and interaction $P^{\rm int}$ contributions to P from the gas to the solid at Pe= 100. Figure adapted from [25].

known to exist [17]. A general scenario was proposed to explain solidification in two dimensions by Halperin, Nelson and Young [18, 19, 20], according to which the ordering transition occurs in two steps: one from the isotropic liquid to a hexatic phase, with short-range translational order and quasi-long-range (QLO) six-fold bond-orientational order, and a second one from the hexatic to the solid, characterized by QLO translational order and a true long-range hexatic one. Both of this two transition are Berezinskii-Kosterlitz-Thouless (BKT) transitions, mediated by unbinding of topological defects. Very recently, numerical simulations [21, 22, 23] and experimental results [24] reached a consistent understanding of the full melting transition for hard disks, which is still a two-step transition, but with a first-order liquid-hexatic transition and a BKT hexatic-solid one.

2. Methods

Active brownian disks model

Active brownian disks constitute the simplest model of self-propelled brownian isotropic particles. The stochastic equations of motion for N repulsively interacting hard disks of mass m, self-propelled by an active force $\mathbf{F}_{\rm act}$ constant in modulus and directed along $\mathbf{n}_i = (\cos\theta_i(t), \sin\theta_i(t))$, are:

$$m\ddot{\mathbf{r}}_i = -\gamma\dot{\mathbf{r}}_i + F_{\rm act}\mathbf{n}_i - \boldsymbol{\nabla}_i \sum_{j(\neq i)}^{N} U(r_{ij}) + \boldsymbol{\xi}_i \ , \qquad \dot{\theta}_i = \eta_i \ , \tag{1}$$

with $\mathbf{r}_i$ the position of the center of the i-th particle, $r_{ij} = |\mathbf{r}_i - \mathbf{r}_j|$ the inter-particle distance. The inter-particle potential is the short-range purely repulsive potential $U(r) = 4\varepsilon[(\sigma/r)^{64} - (\sigma/r)^{32}] + \varepsilon$ if $r < \sigma_d = 2^{1/32}\sigma$, and 0 otherwise, where σ_d is the diameter of the disks.

The terms $\boldsymbol{\xi}$ and η are zero-mean independent Gaussian noises that verify $\langle \boldsymbol{\xi}_i(t)\,\boldsymbol{\xi}_j(t')\rangle = 2\gamma k_B T\delta_{ij}\delta(t-t')\mathbf{1}$, $\langle \eta_i(t)\,\eta_j(t')\rangle = 2D_\theta\delta_{ij}\delta(t-t')$, with $D_\theta = 3k_BT/\gamma\sigma_d^2$. The units of length,

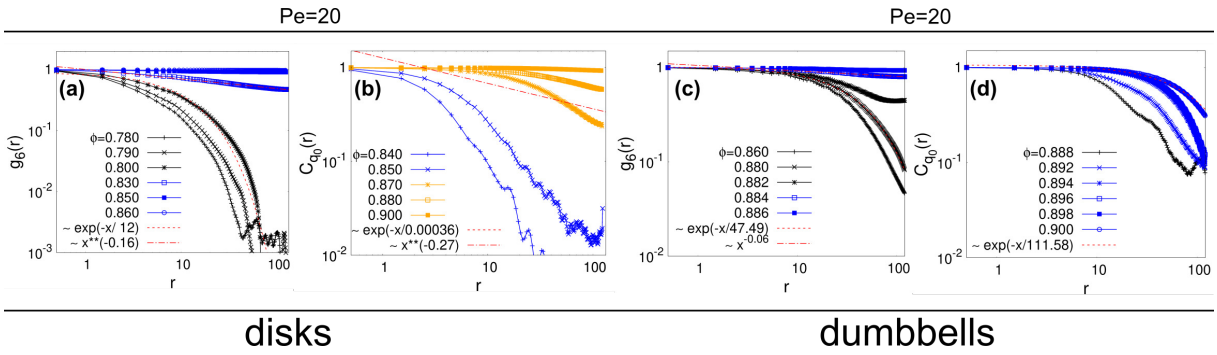

Figure 3. Correlation functions at fixed Pe= 20 and different ϕs as defined in the keys. (a) Hexatic correlations functions for disks across the liquid-hexatic transition; (b) translational correlation functions for disks across the hexatic-solid transition; (c) hexatic correlation functions for dumbbells across the liquid-hexatic transition; (d) translational correlation functions for dumbbells up to the close-packing limit.

mass and energy are given by σ_d, m and ε, and are typically set to one. Two relevant parameter of the model are the surface fraction occupied by the particles $\phi = \pi\sigma_d^2 N/(4V)$, where $V = L^2$ is the system's surface, and the Péclet number $\mathrm{Pe} = F_{\mathrm{act}}\sigma_d/(k_B T)$, which measures the ratio between the work done by the active force and the thermal energy $K_B T$. We tune L and F_{act} at fixed $\gamma = 10$ and $k_B T = 0.05$, according to the value of ϕ and Pe that we want to obtain, in order to explore the whole space parameter. This choice of the values for friction coefficient and temperature ensures the overdamped regime, as commonly used in the field and justified by the low-Re regime of most experiments.

The equation of motions are integrated numerically, using the software LAMMPS [27], with a velocity Verlet algorithm and an additional Langevin-type thermostat. The integration scheme integrated by LAMMPS and carefully described in [28] is a forth-order algorithm for the underdamped equations of motion (1). For the entire portion of parameters' space that we explored, we ensured the dynamics to evolve in a strong viscous regime, being hence safe in disregard all the inertial effects. To be quantitative, a Reynolds number can be defined for our system of active particles, which takes into account the balancing between self-propulsion strength and friction, as follows:

$$Re^{\mathrm{act}} = \frac{\rho L v_0}{\gamma} = \frac{m F_{\mathrm{act}}}{\gamma \sigma_d}, \tag{2}$$

being ρ the density, L the characteristic length of the system which is the diameter σ_d of the disks and $v_0 = F_{\mathrm{act}}/\gamma$. Then, taking care keeping Re^{act} low, both inertia-to-friction (ruled by m/γ) and activity-to-friction ratios would be small enough for all our purposes.

The numerical stability of the integration procedure is instead strongly limited by the ratio between both temperature and self-propulsion force over the pair interaction strength. Particularly for our stiff core interactions, if any of the two leads to some excessive overlaps between two particles within one integration timestep, the potential energy would readily diverge. Both these two instability sources are carefully avoided by choosing a small enough timestep, depending to the temperature and the activity used.

Active dumbbells model
Dumbbells are diatomic molecules consisting of two identical disks of diameter σ_d. The equations of motion for $2N$ disks are:

$$m\ddot{\mathbf{r}}_i = -\gamma\dot{\mathbf{r}}_i + \mathbf{F}_{\rm act} - \boldsymbol{\nabla}_i \sum_{j(\neq i)}^{2N} U(r_{ij}) + \boldsymbol{\chi}_i \ . \tag{3}$$

The potential is the same as the one defined above, while $\boldsymbol{\chi}_i$ are uncorrelated Gaussian noises with zero mean and variance $2\gamma k_B T$. The active force has constant magnitude $F_{\rm act}$ and is kept along the tail-to-head direction. The bond between the disks of each dumbbell are kept rigid at a distance σ_d using a RATTLE scheme [29]. The surface fraction is $\phi = \pi\sigma_d^2(2N)/(4V)$, while the Péclet number is ${\rm Pe} = 2F_{\rm act}\sigma_d/(k_B T)$.
Note that the dumbbell model differ from colloids in the way the rotational diffusion is implemented. While the latter is unaffected by the surrounding particles, because the equation of motion for θ is independent from the atoms positions, dumbbells rotate due to the combination of the noise of the dimers. Thus, when dumbbells start to cluster together, they will not be able to rotate.
The equation of motions are integrated in the same way as the ones of colloids.

3. Phase diagram of the two models

The phase diagram for isotropic particles (Fig. 1(a)) has been established according to a systematic evaluation of several quantities. As described in details in [25], we used local surface fraction pdfs and virial pressure for self-propelled disks defined as in [11] to provide the limits of the coexistence regions throughout the parameters space. Spatial correlation functions $g_6(r)$ for the two-point correlation of the local hexatic parameter $\psi_6(\mathbf{r}_j) = N_j^{-1}\sum_{k=1}^{N_j} e^{{\rm i}6\theta_{jk}}$ and finite size analysis of its 4-th order cumulant allowed us to distinguish between liquid structure and hexatic one, and consequently to locate the liquid-hexatic transition for all values of Pe. Besides, correlation functions $C_{\mathbf{q_0}}(r)$ of local translational order parameter $e^{{\rm i}\mathbf{q_0}\cdot\mathbf{r_i}}$, being $\mathbf{q_0}$ the maximum of the diffraction peak in the reciprocal space, have been used to identify hexatic-solid transition.

It recently came out that a well defined equation of state (EOS) exists also for self-propelled isotropic particles, like the case of our disks. The full strategy to obtain a formulation of the pressure for APBs appeared first in [30]. They proved that, starting from the equation of motion of N self-propelled disks, a virial-like EOS can be constructed, that is well-defined in the sense that Irving and Kirkwood prescribed [31]. This means that the stress tensor extracted from the microscopic equation of motion satisfies the right conservation laws into the corresponding coarse-grained description. The pressure definition that we used is

$$P = \frac{Nk_BT}{V} + \frac{\gamma v_0}{2V}\sum_i \langle \vec{n}_i \cdot \vec{r}_i \rangle + \frac{1}{4V}\sum_{ij} \langle \vec{F}_{ij} \cdot \vec{r}_{ij} \rangle, \tag{4}$$

which only depends on bulk properties of the system and that can thereby be used as an equation of state. The first term is the ideal gas contribution P_0, the third is the virial term $P^{\rm int}$ that accounts for interactions between particles as the system departs from the ideal gas behavior, while the second term $P^{\rm swim}$ is the active term that is usually called *swim pressure*.

The equation of state for zero and weak Pe is shown in Fig. 2(a). $P(\phi)$ is roughly flat in a narrow ϕ interval for Pe$<$ 3. For low activity, the pressure loop well takes into account the co-existence region, as in the standard equilibrium first-order phase transitions (see Fig. 2(b)). Although the equal-area Maxwell construction, that allows to directly extract the binodal cannot be readily applied for Pe$>$ 0, we use it by extension of the passive disks analysis, as a first identification of the coexistence region. Beyond Pe$=$ 3, we do not find evidence for coexistence

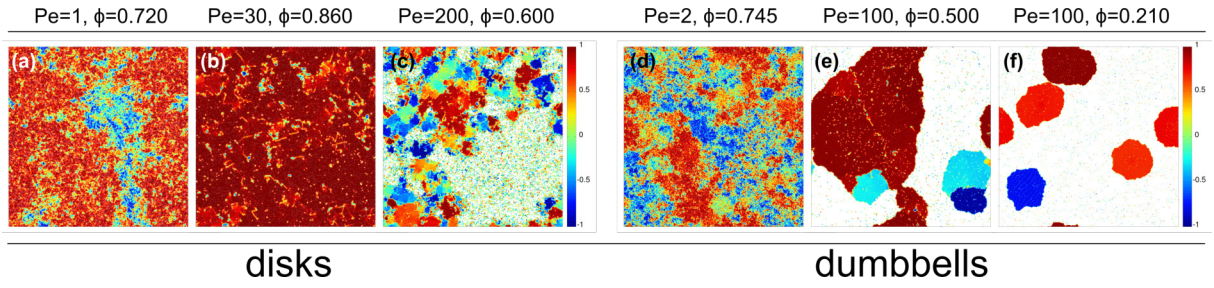

Figure 4. Color representation of the local hexatic parameter ψ_{6j} for disks (left) and dumbbells (right) and for cases given in the labels above the pictures. See the text for details about the color code. The following regions of the phase diagram are shown for disks: (a) liquid-hexatic coexistence at low Pe; (b) hexatic phase at intermediate Pe; (c) MIPS region at high Pe; and for dumbbells: (d) coexistence region at low Pe; (e) MIPS at high Pe, in the middle of the coexistence curve; (f) MIPS at high Pe, close to the lower limit of the coexistence region.

until the high-Pe regime where MIPS is attained. For Pe$>$ 35 the $P(\phi)$ curves become flat in between two densities. Representative curves at $10 \leqslant$ Pe $\leqslant 50$ are displayed in Fig. 2(c). As it has been recently reported, at very high Pe, the pressure drops abruptly at the vicinity of MIPS (see Fig. 2(d)), as a consequence of the existence of a metastability region with a very large nucleation barrier. We obtain the limits of MIPS with an extrapolation of the flat part of $P(\phi)$ across the pressure jump (or spinodal), as illustrated in Fig. 2(d) for Pe$=$ 100.

Both the two peaks structure in density pdfs and the double loop shape in the equation of state consistently demonstrate that the liquid-hexatic transition in the passive limit is a first order phase transition, as expected from repulsive disk with a $\sim r^{-64}$ repulsive interaction [23], and that, notably, the first-order nature of this phase transition is preserved after bringing the system out of equilibrium by adding non-zero small activity, up to Pe$\sim$ 3. For larger Pes liquid-to-hexatic transition undergoes a crossover to a continuous transition. On the other hand, upon increasing activity from the passive limit, the BKT nature of hexatic-solid transition is maintained at all finite activities. Activity has the effect to destabilize the two ordered phases and, as a consequence, hexatic and solid are pushed towards higher surface fraction. Nevertheless, remarkably, both hexatic and solid phases are demonstrated to exist as stable thermodynamic phases up to very high activities. This can be directly observed from the hexatic and translational correlation functions shown, for fixed Pe$=$ 20 in Fig. 3(a,b). Note that above $\phi \gtrsim 0.800$ the hexatic correlation length diverges as expected in the hexatic phase from Halperin-Nelson theory. Above $\phi \gtrsim 0.870$ also the positional correlation length diverges indicating the emergence of quasi-long-range translational order.

Hexatic order for self-propelled disks can also be inferred qualitatively by providing a color map for the local hexatic parameter defined before. We include some examples of this map in Fig. 4 for few representative cases at different points in the Pe-ϕ space reported within the figure. The color scale refers to the projection of the local hexatic parameter along the direction in the complex plane of the sample average of the parameter itself. The specific nature of the configurations shown in Fig. 4 is provided within the caption.

For what concerns dumbbells, we studied the phase diagram in great details in [32, 26], focusing on the emerging relations between the two-dimensional phase transition scheme for passive dumbbells and the motility-induced phase separation. As clearly shown in Fig. 1(b), we found a strongly different, but still much interesting scenario, never seen with disks, demonstrating at least that MIPS is a strong system-dependent phenomenon.

We used the same quantities described above for the disks in order to explore extensively the parameter space. In the limit of passive dumbbells we observed that, similarly to isotropic particles, our molecules undergo a first order phase transition between isotropic liquid and

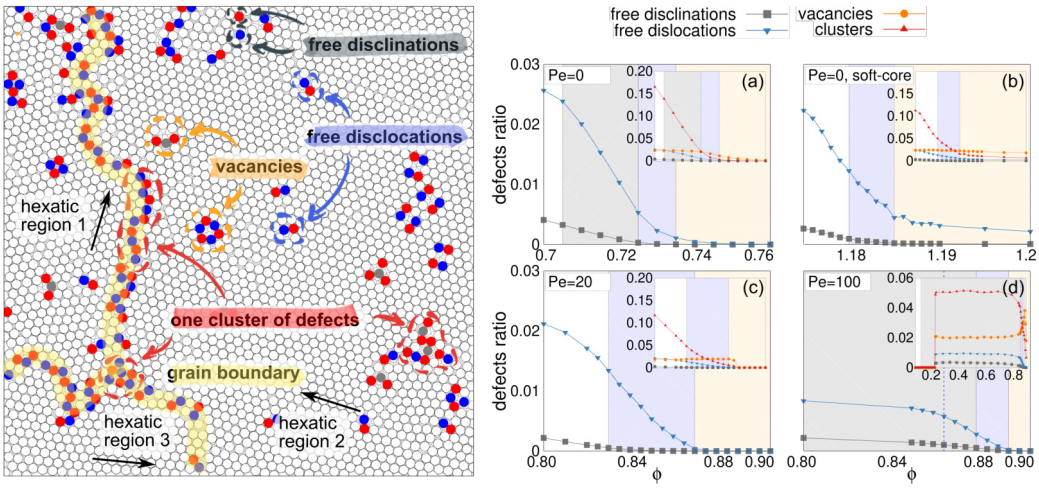

Figure 5. In the left panel a snapshot of one configuration of disks is shown, with all the defects highlighted: free disclinations (in grey) are isolated miscoordinated particles; free dislocations (blue) are 5-fold/7-fold pairs where the usual Burgers vector is directly related with the vector from the 5-fold to the 7-fold particle; vacancies (orange) are usually pairs of dislocation with zero total Burgers vector; grain-boundaries between differently oriented hexatic regions (yellow) contain cluster of defects of arbitrary size with non-zero total Burgers vector. In the right panel populations of all the kind of defects are shown with varying *phi* for the following cases: (a) passive hard-disks; (b) passive soft-disks; (c) Pe20 hard disks; (d) Pe= 100 hard-disks.

a hexatic phase for the mutual orientation of the centers of mass of the single beads. This represents a notable extension to molecular systems of the most recent results obtained for hard disks [22, 24] and is a novelty in the understanding of the nature of 2d melting.

The most remarkable point we found is that, turning on activity and increasing Pe from the passive limit we did not find any finite critical value of activity which triggers the motility-induced phase separation, since we observe macroscopic phase separation for each probed Pe value. As shown in Fig. 3(c), increasing the surface fraction and crossing the upper limit of the coexistence region, quasi-long-range orientational order arises in the system, revealing that coexistence is between a liquid-gas phase and a hexatic phase everywhere in the spanned activity range. Moreover, the finite range of packing fractions where liquid and hexatic coexist is continuously connected throughout the phase diagram, suggesting a crucial interplay between the liquid-hexatic first order phase transition and the motility-induced phase separation.

From both the phase diagram of Fig. 1(b) and translational correlation functions for dumbbells shown in Fig. 3(d) is worth noting that we did not find any certain evidence of the existence of a solid phase for dumbbells. Neither for passive molecules, nor with activity, we observe quasi-long-range positional order for the centers of mass of the beads. As explained in [26], the reason for that comes from the shape of the objects in the system. Indeed, since each head-to-tail distance is fixed to the same value σ_d for all values of the global packing fraction, the beads cannot arrange on a perfect triangular lattice, as they are free to do in the disk geometry, at any global $\phi < \phi_{cp} (\sim 0.900)$.

4. Topological defects in self-propelled disks

After having confirmed that for the active disks model the phase transition scenario is a double-step melting scenario with both the solid-hexatic melting and hexatic-liquid one we remind that in the standard KTHN theory, the two phase transitions are mediated by unbinding of topological defects. Although dislocation pairs don't disrupt the quasi-long-range positional order, they can exist in the solid phase. As free dislocations are excited from unbinding of

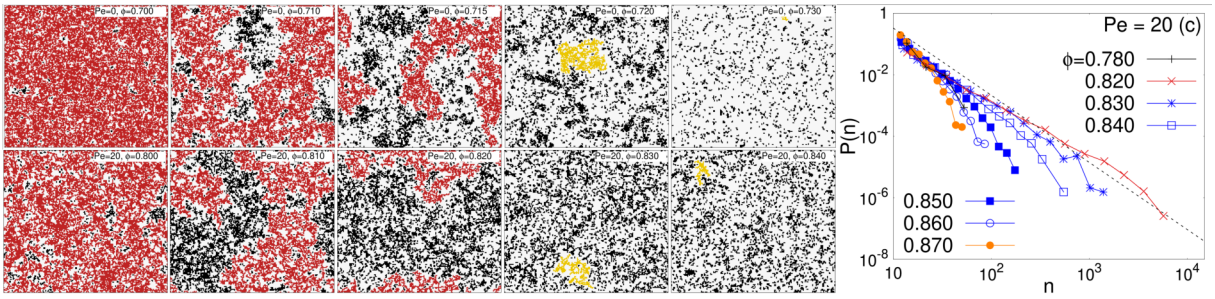

Figure 6. In the left panel percolating behavior of clusters of defects in shown across the liquid-hexatic transition for both a first-order transition at Pe= 0 (first row) and a second-order BKT one at Pe= 20 (second row). On the right, power-law behavior for CSD of the defects clusters at percolation is shown for the case at Pe= 20.

dislocation pairs, the solid melts into the hexatic. Hexatic phase in turn melts in favor of the isotropic liquid with a BKT transition mediated by unbinding of single dislocations into free disclinations, which thus are responsible of destroying the bond-orientational order.

As shown in Fig. 5, we found that this scenario is maintained also for Pe$>$ 0. Even if a theoretical background for interpreting this results still lacks, we can pushed the comparison with the equilibrium Halperin-Nelson theory, saying that we found evidences of the fact that the same topological defects unbinding mechanisms as for the passive case are able to drive a two-step melting scenario also for self-propelled disks.

However, Fig. 5 also shows that among free dislocations and free disclinations, that are supposed to be relevant in the HN-like melting transitions, also a large number of defects clusters are present in the system for all the values of Pe and up to a packing fraction close to the hexatic-solid transition. Clusters of defects are nest-neighbors networks of miscoordinated particles with total non-zero Burgers vector. We studied both the geometrical structure of this clusters of defects and their cluster-size distribution finding that, interestingly, they show a percolating behavior at the liquid-hexatic transition, regardless the transition is first-order or BKT type (see Fig. 6).

Besides a precise characterization of such behavior, we aim to know whether percolation of defects clusters is a ingredient of topological phase transition or not and whether some differences in the percolating behavior, which we didn't observe so far, could give a supplement or perhaps fundamental tool to better understanding the nature of liquid-hexatic transition for both passive and active two dimensional systems.

Conferences and schools

- **FLOWING MATTER 2017**, 23-27th January 2017, PORTO (Portugal).
  Oral contribution "Phase co-existence in bidimensional passive and active dumbbell systems"
- **XXIX SEMINARIO NAZIONALE di FISICA NUCLEARE E SUBNUCLEARE "Francesco Romano"**, 25 Maggio - 1 Giugno 2017, OTRANTO (LE)
- **Liquids 2017 - 10th liquid matter conference**,17-21th July 2017, Ljubljana (Slovenia).
  Poster.
- **The Beg Rohu Summer School - Out of equilibrium dynamics, Evolution and Genetics**, 24 July - 5 August 2017, Beg Rohu (France).
  Lectures: Out of Equilibrium Dynamics of Complex Systems (L.F. Cugliandolo); Evolutionary Dynamics of Large Populations (D.S. Fisher); Counting Equilibria in Complex Systems via Random Matrices (Y.V. Fyodorov); Population Genetics in Space and Time (D.R. Nelson).
- **TAU-ESPCI International Winter School on "Active Matter"**, Jan 28th - Feb 1st 2018, Tel-Aviv (ISRAEL).
  Invited speakers: Roy Beck (Tel Aviv University, Israel), ric Clment (ESPCI, Paris, France), Olivier Dauchot (ESPCI, Paris, France), Vincent Dmery (ESPCI, Paris, France), Luca Giomi (Leiden University, Netherlands), David Hu (Georgia Institute of Technology, USA), Jean-Franois Joanny (ESPCI, Paris, France), Yoav Lahini (Tel Aviv University, Israel), Alexander Leshansky (Technion, Israel), Ayelet Lesman (Tel Aviv University, Israel), Yael Roichman (Tel Aviv University, Israel), Olivia du Roure (ESPCI, Paris, France)
- **International Conference on Computer Simulation in Physics and beyond**, September 24-27, 2018, Moscow (FEDERAZIONE RUSSIA).
  Oral contribution "Melting transition and phase diagram of 2d active hard disks and dumbbells"
- **Erice Workshop on Self-Organization in Active Matter: from Colloids to Cells**, Oct 1-4, 2018, The Ettore Majorana Foundation and Centre for Scientific Culture, Erice (ITALY).
  Oral contribution "Phase Coexistence in Two-dimensional Passive and Active Dumbbell Systems"
- **StatPhys27 - 27th International Conference on Statistical Physics**, Jul 08-12, 2019, Buenos Aires (ARGENTINA)
  Poster "Liquid-hexatic co-existence for 2d self-propelled dumbbells"
- **Physics of Active Matter, StatPhys 2019 Satellite Meeting**, Jul 15-17, 2019, Vina del Mar (CHILE)
  Poster "Passive and active phases of 2d hard disk system"
- **FisMat 2019 - Italian national conference on the physics of matter**, Sep 30 - Oct 04, 2019, Università di Catania, Catania (ITALY)
  Oral contribution

Publications

- L.F. Cugliandolo, P. Digregorio, G. Gonnella, A. Suma, *Phase Coexistence in Two-Dimensional Passive and Active Dumbbell Systems*, Phys. Rev. Lett., **119**, (2017)
- G. Negro, L.N. Carenza, P. Digregorio, G. Gonnella, A. Lamura, *Morphology and flow patterns in highly asymmetric active emulsions*, Physica A: Statistical Mechanics and its Applications, **503**, (2018)
- P. Digregorio, D. Levis, A. Suma, L.F. Cugliandolo, G. Gonnella, I. Pagonabarraga, *Full Phase Diagram of Active Brownian Disks: From Melting to Motility-Induced Phase Separation*, Phys. Rev. Lett., **121**, (2018)
- I. Petrelli, P. Digregorio, L.F. Cugliandolo, G. Gonnella, A. Suma, *Active dumbbells: dynamics and morphology in the coexisting region*, Eur. Phys. J. E **41**, 128 (2018)
- P. Digregorio, D. Levis, A. Suma, L. F. Cugliandolo, G. Gonnella, I. Pagonabarraga, *2D melting and motility induced phase separation in Active Brownian Hard Disks and Dumbbells*, Journal of Physics: Conference Series **1163** (2019)
- G. Negro, L.N. Carenza, P. Digregorio, G. Gonnella, A. Lamura, *In silico characterization of asymmetric active polar emulsions*, AIP Conference Proceedings, **2071**, 1 (2019)

References

[1] Marchetti M C, Joanny J F, Ramaswamy S, Liverpool T B, Prost J, Rao M and Simha R A 2013 *Rev. Mod. Phys.* **85** 1143
[2] Couzin I D and Krause J 2003 *Advances in the Study of Behavior* **32** 1–75
[3] Bialek W, Cavagna A, Giardina I, Mora T, Silvestri E, Viale M and Walczak A M 2012 *Proc. Nat. Ac. Sci. USA* **109** 4786–4791
[4] Zhang H P, Beer A, Florin E L and Swinney H L 2010 *Proc. Nat. Ac. Sci. USA* **107** 13626–13630
[5] Deseigne J, Dauchot O and Chaté H 2010 *Phys. Rev. Lett.* **105** 098001
[6] Bechinger C, Di Leonardo R, Löwen H, Reichhardt C and Volpe G 2016 *Rev. Mod. Phys.* **88** 045006
[7] ten Hagen B, van Teeffelen S and Löwen H 2011 *J. Phys. C: Cond. Matt.* **23** 194119
[8] Romanczuk P, Bär M, Ebeling W, Lindner B and Schimansky-Geier L 2012 *Eur. Phys. J. Spec. Topics* **202** 1–162
[9] Cates M and Tailleur J 2013 *EPL* **101** 20010
[10] Cates M E and Tailleur J 2015 *Annu. Rev. Cond. Matt. Phys.* **6** 219
[11] Levis D, Codina J and Pagonabarraga I 2017 *Soft Matter* **13** 8113–8119
[12] Solon A P, Stenhammar J, Cates M E, Kafri Y and Tailleur J 2018 *Phys. Rev. E* **97** 020602
[13] Bialké J, Speck T and Löwen H 2012 *Phys. Rev. Lett.* **108** 168301
[14] Briand G and Dauchot O 2016 *Phys. Rev. Lett.* **117** 098004
[15] Klamser J U, Kapfer S C and Krauth W 2018 *arXiv:1802.10021*
[16] Mermin N D and Wagner H 1966 *Phys. Rev. Lett.* **17** 1133
[17] Alder B J and Wainwright T E 1962 *Phys. Rev.* **127** 359
[18] Kosterlitz J M and Thouless D J 1973 *J. Phys. C: Solid State Physics* **6** 1181
[19] Halperin B I and Nelson D R 1978 *Phys. Rev. Lett.* **41** 121
[20] Young A 1979 *Phys. Rev. B* **19** 1855
[21] Bernard E P, Krauth W and Wilson D B 2009 *Phys. Rev. E* **80** 056704
[22] Bernard E P and Krauth W 2011 *Phys. Rev. Lett.* **107** 155704
[23] Kapfer S and Krauth W 2015 *Phys. Rev. Lett.* **114** 035702
[24] Thorneywork A L, Abbott J L, Aarts D G A L and Dullens R P A 2017 *Phys. Rev. Lett.* **118** 158001
[25] Digregorio P, Levis D, Suma A, Cugliandolo L F, Gonnella G and Pagonabarraga I 2018 *Phys. Rev. Lett.* **121**(9) 098003
[26] Petrelli, Isabella, Digregorio, Pasquale, Cugliandolo, Leticia F, Gonnella, Giuseppe and Suma, Antonio 2018 *Eur. Phys. J. E* **41** 128
[27] Plimpton S 1995 *J. Comp. Phys.* **117** 1–19
[28] Schneider T and Stoll E 1978 *Phys. Rev. B* **17**(3) 1302–1322
[29] Allen M P and Tildesley D J 1989 *Computer simulation of liquids* (Oxford University Press)
[30] Winkler R G, Wysocki A and Gompper G 2015 *Soft Matter* **11**(33) 6680–6691
[31] Irving J H and Kirkwood J G 1950 *The Journal of Chemical Physics* **18** 817–829
[32] Cugliandolo L F, Digregorio P, Gonnella G and Suma A 2017 *Phys. Rev. Lett.* **119** 268002